Molecular Mechanisms Molecular Docking of Three Mitragyna speciosa Alkaloids with iNOS, TNF-α, and IL-6 and In Silico Toxicity Prediction

Mumya Camary[1*], Binawati Ginting[2], Rosnani Nasution[2] and Bastian Lubis[3]

[1] Doctoral Program in Mathematics and Applied Sciences, Graduate School, Universitas Syiah Kuala, Banda Aceh, Indonesia
[2] Department of Chemistry, Faculty of Mathematics and Natural Sciences, Universitas Syiah Kuala, Banda Aceh, Indonesia
[3] Department of Anesthesiology and Intensive Therapy, Faculty of Medicine, Universitas Sumatera Utara, Medan, Indonesia
dr.mumiya@yahoo.com

Abstract. Sepsis involves a dysregulated host response to infection, in which inflammatory mediators contribute to organ dysfunction. This exploratory study compared the docking scores and predicted interactions of mitragynine, 7-hydroxymitragynine, and speciociliatine with inducible nitric oxide synthase (iNOS; PDB ID 1M8E), tumor necrosis factor-alpha (TNF-α; 6X86), and interleukin-6 (IL-6; 4NI9), together with toxicity predictions from pkCSM and ProTox-III. Within the applied docking protocol, 7-hydroxymitragynine yielded the most negative scores against iNOS (−9.0 kcal/mol) and IL-6 (−9.2 kcal/mol), whereas mitragynine yielded the most negative score against TNF-α (−6.6 kcal/mol). Speciociliatine produced scores of −8.5, −6.1, and −7.5 kcal/mol against iNOS, TNF-α, and IL-6, respectively. pkCSM predicted negative classifications for Ames mutagenici-ty, hERG I inhibition, and skin sensitization for all three compounds, but identified shared hepatotoxicity alerts and predicted hERG II inhibition for mitragynine and speciociliatine. ProTox-III predicted acute oral LD_{50} values of 300 mg/kg for mitragynine and speciociliatine and 1,000 mg/kg for 7-hydroxymitragynine. However, the latter prediction had lower average similarity and prediction accuracy. These findings describe target-dependent computational patterns and predicted toxicity concerns that may inform subsequent experiments. The lack of reported docking protocol validation and experimental confirmation limits confidence in the predicted poses and rankings. The results do not establish binding affinity, functional inhibition, efficacy in sepsis, or safety.

Keywords: Mitragyna speciosa, mitragynine, 7-hydroxymitragynine, speciociliatine, sepsis, iNOS, TNF-α, IL-6, molecular docking, toxicity prediction.

© The Author(s) 2026
F. Maulina and S. Wahyuni (eds.), *Proceedings of the 3rd Malikussaleh International Conference on Health and Disaster Medicine (MICOHEDMED 2026)*, Advances in Health Sciences Research 97,
https://doi.org/10.2991/978-94-6239-836-8_16

1 Introduction

Sepsis is defined as life-threatening organ dysfunction caused by a dysregulated host response to infection. Despite advances in antimicrobials, hemodynamic support, and critical care practice, sepsis remains a major global health problem. Global estimates indicate that sepsis contributes substantially to mortality across age groups and disproportionately affects populations with limited access to timely diagnosis and intensive care [1–3]. The syndrome is biologically heterogeneous and cannot be reduced to uncontrolled inflammation alone; hyperinflammation, endothelial injury, coagulation abnormalities, immunosuppression, metabolic dysfunction, and impaired tissue perfusion can coexist or evolve over time [4–6].

Recognition of infection activates pattern-recognition receptors and downstream transcriptional pathways that promote cytokine and chemokine release. TNF-α is an early inflammatory mediator capable of amplifying leukocyte activation, endothelial adhesion, vascular permeability, and secondary cytokine production [7]. IL-6 integrates innate immune activation with acute-phase and adaptive responses, and circulating IL-6 concentrations frequently track disease severity, although the cytokine also has context-dependent protective and regenerative functions [8,9]. These complexities mean that predicted binding to a cytokine should be interpreted as a mechanistic hypothesis rather than proof that systemic immune dysregulation will be corrected.

Nitric oxide has similar context-dependent actions during infection. Constitutive nitric oxide supports vascular homeostasis and antimicrobial defense, whereas sustained high-output production mediated by iNOS can contribute to vasoplegia, reduced vascular responsiveness, mitochondrial impairment, and heterogeneous microcirculatory flow [10,11]. Complete suppression of nitric oxide may also be harmful because nitric oxide participates in pathogen control and organ perfusion. Accordingly, the computational identification of ligands associated with iNOS must be followed by functional studies that distinguish beneficial modulation from indiscriminate pathway blockade.

Mitragyna speciosa (Korth.) Havil., commonly known as kratom, is a Southeast Asian medicinal plant containing structurally related indole alkaloids. Mitragynine is the predominant alkaloid, whereas 7-hydroxymitragynine is present at lower abundance but exhibits substantial pharmacological activity. Speciociliatine is a stereoisomer of mitragynine that has received increasing attention because its receptor binding, metabolism, and pharmacokinetics differ from those of the major alkaloid [12–16]. Although kratom alkaloids are most widely investigated for opioid-receptor pharmacology, extracts and individual constituents have also shown anti-inflammatory activity in preclinical systems [17,18]. These observations support hypothesis generation but do not establish their usefulness in sepsis.

The translational evaluation of kratom alkaloids requires particular attention to safety. Reported concerns include central nervous system effects, dependence liability, drug–drug interactions, hepatic injury, and cardiovascular events, especially when chemically concentrated products or multiple substances are used [19–22]. Consequently, computational target screening should be integrated with early toxicity prediction rather than interpreted solely from favorable docking scores.

Previous computational studies have examined the effects of kratom alkaloids on inflammatory cytokines. Nuswantoro et al. investigated mitragynine and 7-hydroxymitragynine in a study that included IL-6 and TNF-α, alongside Mycobacterium tuberculosis-related targets [23]. Thus, the investigation of these two alkaloids against IL-6 and TNF-α should not be considered novel. The present study extends this comparative scope by including speciociliatine and iNOS and examining the docking results alongside toxicity predictions from pkCSM and ProTox-III. This study provides an incremental assessment of three structurally related alkaloids across selected inflammation-associated proteins, rather than discovering a previously unrecognized therapeutic mechanism.

Molecular docking generates candidate poses and scores that depend on receptor preparation, search-space definition, and the selected scoring function; these outputs are not experimentally measured binding affinities or evidence of functional inhibition [24]. Accordingly, this study compared the docking scores and predicted contact patterns of mitragynine, 7-hydroxymitragynine, and speciociliatine against iNOS, TNF-α, and IL-6 and examined their toxicity profiles. Sepsis provides the biological context for selecting these proteins; however, computational analysis does not establish efficacy in sepsis. The findings of this study are intended to generate hypotheses for subsequent structural validation and experimental testing.

2 Materials and Methods

2.1 Study Design

A comparative in silico workflow was used, comprising candidate selection, ligand preparation, target-protein preparation, molecular docking, protein–ligand contact analysis, and toxicity prediction. The computational outputs were analyzed descriptively. This study did not involve human participants or experimental animals.

2.2 Selection of Candidate Alkaloids

Mitragynine, 7-hydroxymitragynine, and speciociliatine were selected as structurally related *M. speciosa* alkaloids with documented pharmacological relevance. The three-dimensional structures were obtained from the HMDB and PubChem databases and inspected for chemical identity and stereochemistry before preparation [25,26].

Table 1. Selected *Mitragyna speciosa* alkaloids.

Compound	Database identifier	Study role
Mitragynine	HMDB0041933	Test ligand
7-Hydroxymitragynine	HMDB0247263	Test ligand
Speciociliatine	PubChem CID 15560576	Test ligand

2.3 Ligand Preparation

The ligand structures were converted into the required molecular formats using Open Babel. Hydrogen atoms were added, Gasteiger partial charges were assigned, and rotatable bonds were defined. The prepared ligands were converted to the PDBQT format and visually inspected to identify conversion errors or altered stereochemistry.

2.4 Selection and Preparation of Target Proteins

The crystallographic structures of iNOS oxygenase domain (PDB ID 1M8E), human TNF-α (6X86), and human IL-6 (4NI9) were obtained from the RCSB Protein Data Bank [27]. PDB 1M8E contains 7-nitroindazole within the murine iNOS oxy-genase domain. PDB 6X86 is a human TNF-α structure associated with indolinone compound 11. PDB 4NI9 contains human IL-6 in complex with the modified nucleo-tide aptamer SOMAmer SL1025 [28]. The structures were inspected, unnecessary water molecules and unrelated heteroatoms were removed, polar hydrogens and charg-es were added, and the prepared receptors were converted to PDBQT format.

Table 2. Target proteins and structural references.

Target	PDB ID	Organism	Resolution	Structural reference
iNOS oxygenase domain	1M8E	Mus musculus	2.90 Å	7-Nitroindazole (7NI)
TNF-α	6X86	Homo sapiens	2.93 Å	Indolinone compound 11 (UTY)
IL-6	4NI9	Homo sapiens	2.55 Å	SOMAmer SL1025

2.5 Molecular Docking and Interaction Analysis

Molecular docking was performed using AutoDock Vina [23]. Each alkaloid was docked independently against the prepared iNOS, TNF-α, and IL-6 structures. For each protein–ligand pair, the pose with the most negative docking score and a plausible position within the investigated receptor region was selected for interaction analysis. Docking scores were expressed in kcal/mol, with more negative values interpreted as more favorable predicted binding within the same protocol. The protein–ligand contact residues and two-dimensional interaction maps were examined using BIOVIA Discovery Studio Visualizer software version 2021 (Dassault Systèmes, Vélizy-Villacoublay, France).

2.6 Toxicity Prediction

Canonical molecular representations were submitted to pkCSM to predict Ames mutagenicity, maximum tolerated human dose, hERG I and II inhibition, acute and chronic oral rat toxicity, hepatotoxicity, skin sensitization, Tetrahymena pyriformis toxicity, and minnow toxicity [29]. ProTox-III was used as a complementary platform to estimate acute oral LD_{50}, toxicity class, average similarity, and prediction accuracy [30].

Platform outputs were reported in their original units and interpreted as model-based screening predictions rather than experimentally observed toxicity.

2.7 Data Analysis

Docking scores and toxicity predictions were summarized descriptively. Ligands were compared separately for each protein target within the applied computational protocol. The reported docking scores corresponded to the selected poses and were not treated as independent experimental replicates. No inferential statistical analysis was performed, and numerical differences in docking scores were not interpreted as statistically significant differences in binding affinity or biological potency. Toxicity outputs were interpreted according to their respective endpoints and units, without treating predictions from different platforms as interchangeable experimental measurements.

3 Results

3.1 Molecular Docking Against iNOS

All three alkaloids produced negative docking scores against the iNOS oxygenase-domain structure. 7-Hydroxymitragynine showed the most favorable predicted binding, with a score of −9.0 kcal/mol, followed by speciociliatine at −8.5 kcal/mol and mitragynine at −8.3 kcal/mol. The three ligands shared contacts with residues including TRP188, ARG193, CYS194, ILE195, GLY196, PRO344, ALA345, VAL346, MET349, PHE363, ASN364, GLY365, TRP366, TYR367, MET368, GLU371, TRP457, LEU458, TYR483, and TYR485. The closely related contact profiles indicate occupation of a similar receptor environment under the applied protocol, but they do not establish iNOS inhibition.

Table 3. Docking scores and contact residues against iNOS (PDB ID 1M8E).

Ligand	Score (kcal/mol)	Contact residues
Mitragynine	−8.3	TRP188, ALA191, ARG193, CYS194, ILE195, GLY196, ARG197, SER236, GLN257, PRO344, ALA345, VAL346, MET349, PHE363, ASN364, GLY365, TRP366, TYR367, MET368, THR370, GLU371, ASP376, TRP457, LEU458, PRO461, TYR483, TYR485
7-Hydroxymitragynine	−9.0	TRP188, ALA191, PRO192, ARG193, CYS194, ILE195, GLY196, ARG197, GLN199, LEU203, SER236, PRO344, ALA345, VAL346, MET349, PHE363, ASN364, GLY365, TRP366, TYR367, MET368, GLU371, ARG375, MET428, ALA433, ILE456, TRP457, LEU458, PRO460, PRO461, PHE482, TYR483, TYR485
Speciociliatine	−8.5	TRP188, ALA191, ARG193, CYS194, ILE195, GLY196, GLN257, PRO344, ALA345, VAL346,

MET349, PHE363, ASN364, GLY365, TRP366, TYR367, MET368, GLU371, ARG375, TRP457, LEU458, TYR483, TYR485

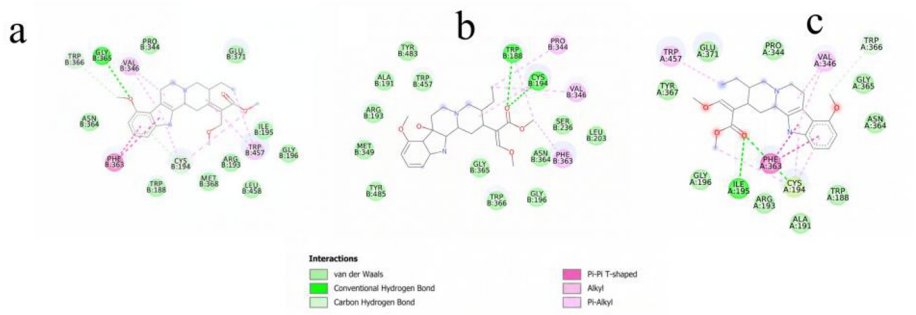


Fig. 1. Molecular docking visualization of iNOS (PDB ID 1M8E): (a) mitragynine, (b) 7-hydroxymitragynine, and (c) speciociliatine. Protein–ligand contact residues and two-dimensional interaction maps were examined using BIOVIA Discovery Studio Visualizer software version 2021 (Dassault Systèmes, Vélizy-Villacoublay, France).

3.2 Molecular Docking Against TNF-α

Mitragynine produced the most favorable docking score against TNF-α, at −6.6 kcal/mol. 7-Hydroxymitragynine and speciociliatine yielded scores of −6.3 and −6.1 kcal/mol, respectively. The numerical range among the alkaloids was narrow. Mitragynine was associated with a residue environment extending from ASN61–LEU64 and LEU92–GLN127 to THR137–LEU148. The other two alkaloids contacted residues from chains A and C, with repeated contacts involving GLU99, GLN102, ASN103, GLU106, GLU109, GLU110, ARG113, ALA114, GLN116, MET117, SER118, and LYS120. These results suggest predicted interaction with TNF-α but do not demonstrate disruption of trimerization or receptor binding.

Table 4. Docking scores and contact residues against TNF-α (PDB ID 6X86).

Ligand	Score (kcal/mol)	Contact residues
Mitragynine	−6.6	ASN61, LEU62, ASN63, LEU64, PRO65, LEU92, GLU93, GLU95, VAL96, TYR97, GLU99, GLN116, LYS120, ILE123, GLN127, THR137, THR138, PRO139, ASP140, PRO141, THR142, THR143, ASN144, ALA145, SER146, LEU147, LEU148
7-Hydroxymitragynine	−6.3	Chain A: GLN28, TYR31, GLU99, GLN102, ASN103, ARG104, PHE105, GLU106, GLU109, GLU110, ALA112, ARG113, ALA114, GLN116, MET117, SER118, LYS120, VAL121. Chain C:

		GLU99, GLN102, ASN103, GLU106, GLU109, GLU110, ARG113, ALA114, GLN116, MET117, SER118, LYS120
Speciociliatine	−6.1	Chain A: TYR31, ALA38, GLU99, GLN102, ASN103, PHE105, GLU106, SER107, SER108, GLU109, GLU110, GLN111, ARG113, ALA114, GLN116, MET117, SER118, LYS120. Chain C: GLU99, GLN102, ASN103, GLU109, GLU110, ARG113, GLN116, MET117, LYS120

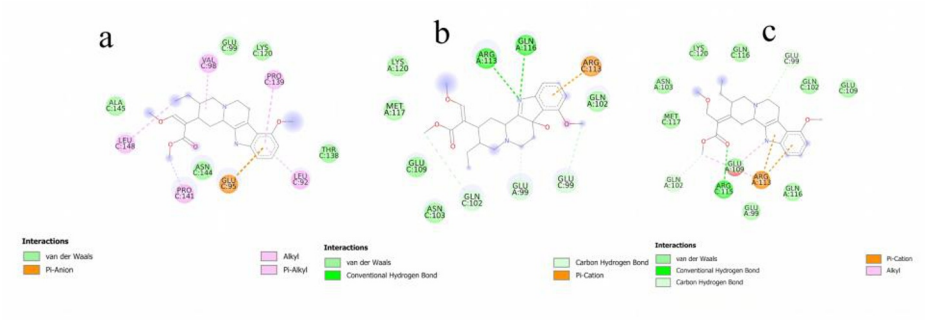


Fig. 2. Molecular docking visualization of TNF-α (PDB ID 6X86): (a) mitragynine, (b) 7-hydroxymitragynine, and (c) speciociliatine. Protein–ligand contact residues and two-dimensional interaction maps were examined using BIOVIA Discovery Studio Visualizer software version 2021 (Dassault Systèmes, Vélizy-Villacoublay, France).

3.3 Molecular Docking Against IL-6

7-Hydroxymitragine produced the most favorable IL-6 docking score, at −9.2 kcal/mol. Mitragynine and speciociliatine each yielded −7.5 kcal/mol. All three alkaloids contacted residues distributed across chains A, B, D, and F. Repeated contacts included GLU53, ARG82, VAL91, GLU127, PHE144, ALA145, GLU146, and SER147. Because 4NI9 is an IL-6 complex with a large modified nucleotide aptamer rather than a conventional small-molecule inhibitor, these results should be described as predicted interactions with the investigated IL-6 structural region and not as direct replication of SOMAmer binding or proof of IL-6 neutralization.

Table 5. Docking scores and contact residues against IL-6 (PDB ID 4NI9).

Ligand	Score (kcal/mol)	Contact residues
Mitragynine	−7.5	Chain A: GLU53, GLY54, LEU55, ARG82, VAL91, VAL123, PHE124, GLN125, GLU127. Chain B: HIS15, VAL17, GLU23, LYS65, GLY66, ASP140, TYR141, LEU142, ASP143, PHE144, ALA145, SER147, GLY148, GLN149. Chain D: PRO20, ARG32, ALA33, PHE144, ALA145, GLU146,

		SER147. Chain F: GLU53, ARG82, ALA84, VAL85, SER86, TYR87, THR89, VAL91, GLU127, LYS128, GLY129, ASP130
7-Hydroxymitragynine	−9.2	Chain A: GLU53, LEU55, ARG82, ALA84, THR89, VAL91, ASN92, LEU93, VAL123, PHE124, GLN125, GLU127. Chain B: VAL17, ALA18, PRO20, GLN21, GLU23, LEU142, ASP143, PHE144, ALA145, GLU146, SER147, GLY148, GLN149. Chain D: PRO20, ARG31, ARG32, ALA33, ASN34, ALA35, LEU36, PHE144, ALA145, GLU146, SER147. Chain F: GLU53, ARG82, ALA84, VAL85, SER86, TYR87, THR89, LYS90, VAL91, ASN92, GLN125, LEU126, GLU127, LYS128, ASP130
Speciociliatine	−7.5	Chain A: GLU53, LEU55, ARG82, VAL123, PHE124, GLN125, LEU126, GLU127. Chain B: VAL17, PRO20, GLU23, LYS65, GLY66, GLN67, ASP140, TYR141, LEU142, ASP143, PHE144, ALA145, GLU146, SER147, GLY148, GLN149. Chain D: PRO20, ARG31, ARG32, ALA33, PHE144, ALA145, GLU146, SER147. Chain F: GLU53, ARG82, ALA84, VAL85, SER86, TYR87, THR89, LYS90, VAL91, GLU127, LYS128, ASP130

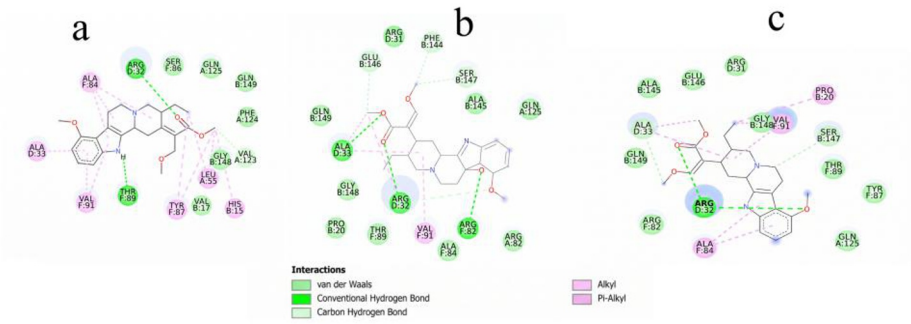


Fig. 3. Molecular docking visualization of IL-6 (PDB ID 4NI9): (a) mitragynine, (b) 7-hydroxymitragynine, and (c) speciociliatine. The protein–ligand contact residues and two-dimensional interaction maps were examined using BIOVIA Discovery Studio Visualizer software (version 2021; Dassault Systèmes, Vélizy-Villacoublay, France).

3.4 pkCSM Toxicity Predictions

All three alkaloids were predicted to be negative for Ames mutagenicity, hERG I inhibition, and skin sensitization. Mitragynine and speciociliatine were predicted to be hERG II inhibitors, whereas 7-hydroxymitragynine was negative for this endpoint. All three compounds generated positive hepatotoxicity predictions. The predicted maximum tolerated human doses were −0.450, −0.466, and −0.406 log mg/kg/day for mitragynine, 7-hydroxymitragynine, and speciociliatine, respectively. These findings represent computational safety alerts rather than experimentally confirmed toxic effects.

Table 6. pkCSM toxicity predictions.

Endpoint	Mitragynine	7-Hydroxymitragynine	Speciociliatine	Unit
Ames toxicity	No	No	No	Categorical
Maximum tolerated dose (human)	−0.450	−0.466	−0.406	log mg/kg/day
hERG I inhibitor	No	No	No	Categorical
hERG II inhibitor	Yes	No	Yes	Categorical
Oral rat acute toxicity (LD_{50})	3.157	2.954	2.967	mol/kg
Oral rat chronic toxicity (LOAEL)	0.311	1.580	−0.108	log mg/kg bw/day
Hepatotoxicity	Yes	Yes	Yes	Categorical
Skin sensitization	No	No	No	Categorical
T. pyriformis toxicity	0.783	0.503	0.902	log µg/L
Minnow toxicity	−0.763	0.912	0.488	log mM

3.5 ProTox-III Toxicity Predictions

ProTox-III returned predicted acute oral LD_{50} values of 300 mg/kg for mitragynine and speciociliatine, with both compounds assigned to toxicity class 3. The average similarity and prediction accuracy were 65.55% and 68.07%, respectively. For 7-hydroxymitragynine, the predicted LD_{50} was 1,000 mg/kg, corresponding to toxicity class 4, with an average similarity of 47.59% and a prediction accuracy of 54.26%. These values are platform-reported prediction outputs, rather than experimental measurements. Although 7-hydroxymitragynine received a less severe predicted acute-toxicity classification, its lower similarity and prediction accuracy substantially limit confidence in the comparative interpretation. Therefore, the results do not establish that 7-hydroxymitragynine is safer than the other alkaloids.

Table 7. ProTox-III acute toxicity predictions.

Compound	Predicted LD_{50}	Toxicity class	Average similarity	Prediction accuracy
Mitragynine	300 mg/kg	3	65.55%	68.07%
7-Hydroxymitragynine	1,000 mg/kg	4	47.59%	54.26%
Speciociliatine	300 mg/kg	3	65.55%	68.07%

4 Discussion

This study identified target-dependent differences in the predicted binding of three M. speciosa alkaloids. 7-Hydroxymitragynine showed the most favorable scores against iNOS and IL-6, whereas mitragynine ranked first against TNF-α. Speciociliatine remained close to mitragynine against iNOS but produced the least favorable score against TNF-α and matched mitragynine against IL-6. These results support different

prioritization for each target rather than the selection of a single universally superior alka-loid. The findings are exploratory and cannot establish inhibition of cytokine sig-nal-ing, suppression of nitric oxide production, or therapeutic activity in sepsis.

The iNOS results produced the clearest separation among the three compounds, with 7-hydroxymitragynine reaching −9.0 kcal/mol. All ligands contacted a broadly shared residue environment containing TRP188, ARG193, CYS194, ILE195, GLY196, PRO344, ALA345, VAL346, MET349, PHE363, ASN364, GLY365, TRP366, TYR367, MET368, GLU371, TRP457, LEU458, TYR483, and TYR485. The addi-tional hydroxyl group of 7-hydroxymitragynine may alter its polarity, hydrogen-bond-ing potential, and pose orientation relative to mitragynine. Nevertheless, contact residue similarity and a favorable score do not indicate that catalytic nitric-oxide production is reduced. Enzyme assays measuring nitric oxide or citrulline synthesis are required.

iNOS is mechanistically relevant to septic vasoplegia because inflammatory signal-ing can induce sustained nitric oxide production, reduce vascular responsiveness, and contribute to mitochondrial and microcirculatory dysfunction [10,11]. However, nitric oxide also supports antimicrobial defense and endothelial signaling. Previous attempts at non-selective nitric oxide synthase inhibition in septic shock illustrate the risk of assuming that pathway suppression is uniformly beneficial [31]. Accordingly, the pre-sent results should motivate concentration-dependent functional studies rather than a direct claim that 7-hydroxymitragynine would improve blood pressure or survival.

Against TNF-α, mitragynine produced the most negative score, but the differences among compounds were only 0.3–0.5 kcal/mol. Such small differences fall within the uncertainty expected from docking scoring functions and should not be interpreted as robust evidence of superior potency [24]. TNF-α functions as a trimer and interacts with large receptor surfaces; successful small-molecule modulation may require occupation of an intersubunit pocket, alteration of trimer stability, or interference with receptor-binding geometry [32]. Contact with TNF-α alone therefore does not demon-strate neu-tralization of cytokine signaling. Biophysical binding assays and TNF-responsive cell systems are needed to test whether mitragynine changes receptor activation.

The IL-6 result for 7-hydroxymitragynine was the most favorable score observed in this study. Repeated contacts across the three alkaloids included GLU53, ARG82, VAL91, GLU127, PHE144, ALA145, GLU146, and SER147. The 4NI9 structure pro-vides useful information about a ligand-accessible IL-6 surface, but its crystallographic partner is SOMAmer SL1025, a modified nucleic acid ligand that engages an extended surface overlapping receptor-binding regions [28]. A small alkaloid cannot be assumed to reproduce the multivalent binding mode of this aptamer. The docking score should consequently be interpreted as predicted local complementarity, not evidence that IL-6Rα or gp130 recruitment is blocked.

IL-6 has pleiotropic actions in infection. Classical and trans-signaling pathways reg-ulate acute-phase responses, leukocyte trafficking, endothelial activation, and immune cell differentiation [8,9]. High circulating IL-6 is frequently associated with greater se-verity, but the cytokine also contributes to host defense and tissue repair. A compound that binds IL-6 weakly or at a nonfunctional surface may have no measura-ble effect on signaling. Appropriate validation would include direct binding analysis, IL-6–IL-

6Rα competition, gp130-dependent reporter assays, and measurement of downstream JAK/STAT activation.

The biological literature on M. speciosa provides a rationale for investigating inflammatory mechanisms but remains insufficient for anti-sepsis claims. An early experimental study reported the anti-inflammatory activity of M. speciosa leaf extract, and later work has described the modulation of inflammatory mediators by mitragynine or kratom-derived preparations [17,18]. Extract-level findings cannot be automatically assigned to a single alkaloid because botanical preparations contain multiple constituents and may vary with chemotype, geography, harvest, processing, and extraction. Moreover, anti-inflammatory activity in chemically induced inflammation does not necessarily predict efficacy in infection-driven organ dysfunction.

The overlap with previous computational work also limits the novelty of the present findings. Nuswantoro et al. included IL-6 and TNF-α in their investigation of mitragynine and 7-hydroxymitragynine [23]. The present study adds speciociliatine and iNOS to the comparison and considers predicted toxicity alongside docking out-comes. These additions broaden the assessment but do not establish a new mecha-nism of action. Numerical docking scores from separate studies should not be inter-preted as directly comparable unless receptor preparation, binding-site definition, scoring functions, and search settings are sufficiently aligned. The present results therefore require validation within their own computational protocol rather than con-firmation through apparent agreement with previously published rankings.

7-Hydroxymitragine is pharmacologically distinct from mitragynine despite their close structural relationship. It exhibits strong opioid receptor activity and can also be formed metabolically from mitragynine [14,15]. Thus, prioritizing 7-hydroxymitragynine on docking grounds introduces neurological, respiratory, depend-ence, and exposure considerations that are not captured by the selected toxicity end-points. The best-scoring ligand may not be the most suitable candidate if its effective exposure overlaps with central opioid effects. Target-engagement studies should therefore be combined with receptor selectivity, respiratory safety, and behavioral evaluation.

Speciociliatine also warrants separate consideration. It is a stereoisomer of mitragynine with distinct opioid-binding, metabolism, and pharmacokinetic characteristics [16,33]. Its relatively favorable iNOS score indicates that minor or less-studied kratom alkaloids should not be excluded from mechanistic screening. Conversely, the positive hERG II and hepatotoxicity predictions mean that further development would require explicit cardiac and hepatic safety evaluation. Structural similarity does not guarantee identical disposition or toxicity among the three alkaloids.

The pkCSM findings identified hepatotoxicity as a shared alert and hERG II inhibition as a compound-dependent concern. Hepatotoxicity is clinically relevant because kratom-associated liver injury has been reported, although causality can be complicated by product composition, contaminants, dose, and co-exposures [19–22]. The computational result cannot determine the mechanism, incidence, or exposure threshold. Hepatocyte assays, bile-acid transport studies, reactive-metabolite assessment, and repeated-dose studies would be needed to characterize the signal.

The predicted hERG II inhibition for mitragynine and speciociliatine deserves attention because blockade of the Kv11.1 channel can delay repolarization and increase

proarrhythmic risk [34]. A binary model classification is not equivalent to an experimentally measured concentration–response relationship. Patch-clamp testing should be interpreted alongside unbound systemic concentrations, active metabolites, and effects on other cardiac ion channels. This is particularly important in sepsis, where electrolyte disturbances, organ dysfunction, and interacting medications may already increase arrhythmia risk.

The ProTox-III results indicate differences in model-predicted acute toxicity but do not establish comparative experimental safety. In particular, the 47.59% average similarity and 54.26% prediction accuracy reported for 7-hydroxymitragynine warrant caution when interpreting its higher predicted LD_{50}. These platform-reported metrics should not be interpreted as the probability that the compound is safe. Furthermore, acute lethality predictions do not resolve hepatic, cardiac, neurological, respiratory, or dependence-related concerns. The pkCSM and ProTox-III outputs also represent distinct models and endpoint conventions and should not be compared numerically without confirming their units and transformations [29,30]. Similar predictions for stereoisomers cannot independently confirm that stereochemistry was preserved or that the models adequately distinguish stereochemistry-dependent toxicity.

Receptor models represent individual crystallographic conformations, whereas proteins in biological systems are dynamic and influenced by the solvent, ions, post-translational modifications, oligomeric state, and interacting partners. Conventional docking incompletely captures induced fit, water-mediated interactions, entropy, and intracellular exposure [23,24]. The selected targets represent only a part of the sepsis network, and no computational result can reproduce the temporal transition between hyperinflammation and immunosuppression. Finally, toxicity predictions do not fully account for metabolism, mixture effects, formulation, dose, or critical illness physiology.

A rational validation sequence would begin with biochemical or biophysical target-binding experiments, followed by iNOS activity measurements and TNF-α or IL-6-responsive cellular assays. Compounds that show functional activity should then undergo cytotoxicity, hepatocyte, hERG, metabolic stability, plasma protein binding, and permeability evaluations. Only candidates with an acceptable exposure–safety relationship should progress to infection-relevant cellular systems and appropriately designed animal models of sepsis.

5 Conclusion

This exploratory study reports docking-score patterns and predicted toxicity profiles for three M. speciosa alkaloids evaluated against iNOS, TNF-α, and IL-6. Although 7-hydroxymitragynine yielded the most negative reported scores against iNOS and IL-6, and mitragynine against TNF-α, these numerical rankings do not establish pharmacological superiority. Unresolved questions concerning receptor preparation, binding-site relevance, and docking reproducibility limit confidence in compound prioritization. The toxicity predictions identify potential concerns but do not demonstrate comparative safety. The findings should therefore be regarded as hypotheses requiring structural verification, docking protocol validation, and direct experimental testing before conclusions about target inhibition or efficacy in sepsis can be drawn.

Acknowledgments. The authors gratefully acknowledge Universitas Syiah Kuala and Universitas Sumatera Utara, Indonesia, for their institutional and academic support during this study.

Disclosure of Interests. The authors declare no competing interests relevant to the content of this study.

References

1. Singer, M., Deutschman, C.S., Seymour, C.W., et al.: The Third International Consensus Definitions for Sepsis and Septic Shock (Sepsis-3). JAMA 315, 801–810 (2016).
2. Rudd, K.E., Johnson, S.C., Agesa, K.M., et al.: Global, regional, and national sepsis incidence and mortality, 1990–2017. Lancet 395, 200–211 (2020).
3. Evans, L., Rhodes, A., Alhazzani, W., et al.: Surviving Sepsis Campaign: international guidelines for management of sepsis and septic shock 2021. Intensive Care Med. 47, 1181–1247 (2021).
4. Cecconi, M., Evans, L., Levy, M., Rhodes, A.: Sepsis and septic shock. Lancet 392, 75–87 (2018).
5. van der Poll, T., Shankar-Hari, M., Wiersinga, W.J.: The immunology of sepsis. Immunity 54, 2450–2464 (2021).
6. Hotchkiss, R.S., Moldawer, L.L., Opal, S.M., Reinhart, K., Turnbull, I.R., Vincent, J.L.: Sepsis and septic shock. Nat. Rev. Dis. Primers 2, 16045 (2016).
7. Bradley, J.R.: TNF-mediated inflammatory disease. J. Pathol. 214, 149–160 (2008).
8. Tanaka, T., Narazaki, M., Kishimoto, T.: IL-6 in inflammation, immunity, and disease. Cold Spring Harb. Perspect. Biol. 6, a016295 (2014).
9. Hunter, C.A., Jones, S.A.: IL-6 as a keystone cytokine in health and disease. Nat. Immunol. 16, 448–457 (2015).
10. Cinelli, M.A., Do, H.T., Miley, G.P., Silverman, R.B.: Inducible nitric oxide synthase: regulation, structure, and inhibition. Med. Res. Rev. 40, 158–189 (2020).
11. Cauwels, A.: Nitric oxide in shock. Kidney Int. 72, 557–565 (2007).
12. Hassan, Z., Muzaimi, M., Navaratnam, V., et al.: From Kratom to mitragynine and its derivatives: physiological and behavioural effects. Neurosci. Biobehav. Rev. 37, 138–151 (2013).
13. Kruegel, A.C., Grundmann, O.: The medicinal chemistry and neuropharmacology of kratom. Neuropharmacology 134, 108–120 (2018).
14. Kruegel, A.C., Gassaway, M.M., Kapoor, A., et al.: Synthetic and receptor signaling explorations of the Mitragyna alkaloids. J. Am. Chem. Soc. 138, 6754–6764 (2016).
15. Obeng, S., Kamble, S.H., Reeves, M.E., et al.: Investigation of the adrenergic and opioid binding affinities, metabolic stability, plasma protein binding properties, and functional effects of selected indole-based kratom alkaloids. J. Med. Chem. 63, 433–439 (2020).
16. Kamble, S.H., Berthold, E.C., Raju, K.S.R., et al.: Metabolism of speciociliatine, an overlooked kratom alkaloid for its potential pharmacological effects. AAPS J. 24, 86 (2022).
17. Shaik Mossadeq, W.M., Sulaiman, M.R., Tengku Mohamad, T.A., et al.: Anti-inflammatory and antinociceptive effects of *Mitragyna speciosa* Korth methanolic extract. Med. Princ. Pract. 18, 378–384 (2009).

18. Rahmawati, S.I., Indriani, D.W., Ningsih, F.N., et al.: Dual anti-inflammatory activities of COX-2/5-LOX driven by kratom alkaloid extracts in lipopolysaccharide-induced RAW 264.7 cells. Sci. Rep. 14, 28993 (2024).
19. Warner, M.L., Kaufman, N.C., Grundmann, O.: The pharmacology and toxicology of kratom: from traditional herb to drug of abuse. Int. J. Legal Med. 130, 127–138 (2016).
20. Meireles, V., Rosado, T., Barroso, M., et al.: *Mitragyna speciosa*: clinical, toxicological aspects and analysis in biological and non-biological samples. Medicines 6, 35 (2019).
21. Tanna, R.S., Nguyen, J.T., Hadi, D.L., et al.: Clinical pharmacokinetic assessment of kratom (*Mitragyna speciosa*), a botanical product with opioid-like effects, in healthy adult participants. Pharmaceutics 14, 620 (2022).
22. McCurdy, C.R., Sharma, A., Smith, K.E., et al.: An update on the clinical pharmacology of kratom: uses, abuse potential, and future considerations. Expert Rev. Clin. Pharmacol. 17, 131–142 (2024).
23. Nuswantoro A, Nugraha J, Sudjarwo SA, Rejeki PS, Aprillia D. In silico anti-tuberculosis and immunomodulatory effect of mitragynine. Trop J Pharm Res. 2026;25(2):161-170.
24. Warren, G.L., Andrews, C.W., Capelli, A.M., et al.: A critical assessment of docking programs and scoring functions. J. Med. Chem. 49, 5912–5931 (2006).
25. Wishart, D.S., Guo, A., Oler, E., et al.: HMDB 5.0: the Human Metabolome Database for 2022. Nucleic Acids Res. 50, D622–D631 (2022). https://doi.org/10.1093/nar/gkab1062
26. Kim, S., Chen, J., Cheng, T., et al.: PubChem 2023 update. Nucleic Acids Res. 51, D1373–D1380 (2023).
27. Berman, H.M., Westbrook, J., Feng, Z., et al.: The Protein Data Bank. Nucleic Acids Res. 28, 235–242 (2000).
28. Gelinas, A.D., Davies, D.R., Edwards, T.E., et al.: Crystal structure of interleukin-6 in complex with a modified nucleic acid ligand. J. Biol. Chem. 289, 8720–8734 (2014).
29. Pires, D.E.V., Blundell, T.L., Ascher, D.B.: pkCSM: predicting small-molecule pharmacokinetic and toxicity properties. J. Med. Chem. 58, 4066–4072 (2015). https://doi.org/10.1021/acs.jmedchem.5b00104
30. Banerjee, P., Kemmler, E., Dunkel, M., Preissner, R.: ProTox 3.0: a webserver for toxicity prediction. Nucleic Acids Res. 52, W513–W520 (2024).
31. López, A., Lorente, J.A., Steingrub, J., et al.: Multiple-center, randomized, placebo-controlled, double-blind study of the nitric oxide synthase inhibitor 546C88: effect on survival in patients with septic shock. Crit. Care Med. 32, 21–30 (2004).
32. He, M.M., Smith, A.S., Oslob, J.D., et al.: Small-molecule inhibition of TNF-α. Science 310, 1022–1025 (2005).
33. Berthold, E.C., Kamble, S.H., Raju, K.S.R., et al.: Preclinical pharmacokinetic study of speciociliatine in rats. J. Pharm. Biomed. Anal. 194, 113778 (2021).
34. Vandenberg, J.I., Perry, M.D., Perrin, M.J., Mann, S.A., Ke, Y., Hill, A.P.: hERG K+ channels: structure, function, and clinical significance. Physiol. Rev. 92, 1393–1478 (2012).

Open Access This chapter is licensed under the terms of the Creative Commons Attribution-NonCommercial 4.0 International License (http://creativecommons.org/licenses/by-nc/4.0/), which permits any noncommercial use, sharing, adaptation, distribution and reproduction in any medium or format, as long as you give appropriate credit to the original author(s) and the source, provide a link to the Creative Commons license and indicate if changes were made.

The images or other third party material in this chapter are included in the chapter's Creative Commons license, unless indicated otherwise in a credit line to the material. If material is not included in the chapter's Creative Commons license and your intended use is not permitted by statutory regulation or exceeds the permitted use, you will need to obtain permission directly from the copyright holder.

